APPLICATION OF A CROSS-CORRELATION TECHNIQUE IN ULTRASONIC FATIGUE DETECTION

by

Kin-Ping Moy

Submitted in Partial Fulfillment of the Requirements

for the Degree of

Master of Science in Engineering

in the

Electrical Engineering

Program

Allan J. Zuckerman 5/30/73

Adviser Date

Carl E. Kill May 30, 1973

Dean of the Graduate School Date

YOUNGSTOWN STATE UNIVERSITY

June, 1973

ABSTRACT

APPLICATION OF A CROSS CORRELATION TECHNIQUE IN ULTRASONIC FATIGUE DETECTION

Kin-Ping Moy

Master of Science in Engineering

Youngstown State University, 1973

The objective of this thesis is to establish the groundwork of ultrasonic signature analysis for fatigue detection in complex structures. Ultrasonic pulses are transmitted into a simple solid specimen with simulated defect, and are detected by a receiving transducer located at a strategic position. The cross power spectrum of the signals at transmitting and receiving transducers is calculated and found to be very sensitive to the size of the defect and useful in noise elimination.

ACKNOWLEDGEMENTS

The author would like to express his graditude to Dr. Allan J. Zuckerwar, his principal adviser, professor of the Electrical Engineering Department, Youngstown State University, for his continuous assistance throughout the preparation, development and completion of the thesis.

The author is also thankful to Professor Samuel J. Skarote and Dr. Robert H. Foulkes, Jr. for their valuable suggestions; and to Anna Mae Serrecchio for typing the manuscript.

The author wishes to acknowledge that this thesis is prepared under the NASA Grant NGR 36-028-006.

TABLE OF CONTENTS

Page

LIST OF FIGURES

GLOSSARY OF SYMBOLS

a = Pulse width

A_m = Fourier-Bessel coefficient in expression of scattered wave

B_m = Radiation amplitude for a cylinder

c = Wave velocity of ultrasound

C_n = Constant of Fourier Series (See page 9)

e = 2.71828 .... Base of natural logarithms

f_o = Frequency of ultrasound

$G_{SR}(f)$ = Cross power spectrum

i = Square root of -1

I = Intensity of ultrasound

$J_m(x)$ = Bessel function

k = Wave number of ultrasound

m = Order of Bessel and Neumann Functions

n = Harmonic index of ultrasonic pulse

$n(t)$ = Random noise

$N_m(x)$ = Neumann function

p_o = Initial pressure pulse amplitude

p_p = Incident plane wave pressure amplitude

p_s = Scattered wave pressure amplitude

p_T = Total wave pressure amplitude

$\langle p_T \rangle$ = Average of total wave pressure amplitude

r = Radial distance from origin

r_o = Radius of cylindrical hole

$\underline{R}(f)$ = Receiving pulse in frequency domain

$R(t)$ = Receiving pulse in time domain

$\mathrm{sinc}(x)$ = Sinc function (See page 11)

$\underline{S}(f)$ = Transmitted pulse in frequency domain

$S(t)$ = Transmitted pulse in time domain

$S(\phi)$ = Scattered intensity ratio

t = Time

T_o = Period of transmitted pulses

T_R = Transit time of ultrasonic pulses

$\delta(x)$ = Impulse function

E_m = Neumann symbol (See page 15)

η = Attenuation factor

θ_m = Phase shift for cylindrical scattering

λ = Wavelength of ultrasound

Λ = Variable used to define impulse function (Appendix A)

ρ = Density of medium

τ = Phase shift in cross-correlation

ϕ = Axial angle for cylindrical coordinates

$\phi_{SR}(t)$ = Cross-correlation function

$\psi_S(\phi)$ = Angular part of scattered intensity

ω = Angular velocity of ultrasound

I INTRODUCTION

A. Statement of the Problem.

The project is to investigate the method of ultrasonic signature analysis for fatigue detection in complex structures. Fatigue may be defined as deterioration of the mechanical strength of a material or structure to the point of fracture under repeated loads. At the present time, crack detection for complex structure is only limited to visual and dye-check methods. Sometimes the crack located in inaccessible parts of the structure remains unnoticed, and thus, a more improved method will have to be developed.

B. Conventional Methods in Non-destructive Testing.

Some of the more practical and commonly used method are described below:

1. Electromagnetic
   a. Microwave signature analysis [1].
   b. Direct-view radiology [2a].
   c. Infrared thermography [2b].
2. Optical
   a. Spitial filtering [3].
   b. T.V. crack detection [4].
3. Magnetic
   a. Magnetic perturbation [5,6].
   b. Magnetic rubber inspection [7].
4. Acoustic Emission [8].

5. Eddy current [2c].
6. Ames signature analysis [9].
7. Ultrasonic
   a. Ultrasonic spectroscopy [2d].
   b. Ultrasonic imaging [2e].
   c. Ultrasonic critical-angle reflectivity [2f].
   d. Ultrasonic holography [2g].

C. Criteria of non-destructive testing for complex structures.

In order to achieve satisfactory results, non-destructive testing system must fulfill the following criteria:

1. Adapatability to complex structures.
   The system must be able to measure fatigue in a complex structure rather than simple laboratory model.
2. Depth of interrogation.
   The system must be able to detect the flaws within the interior of the structure as well as the surface.
3. Nature of excitation and power availability.
   A system that can respond to externally introduced flux is more desirable than the one that generates its own response signal.

In order for the present methods to work, the source of energy, the geometry of the specimen, and nature of the structure must be carefully controlled, and they cannot satisfy all three of the criteria. On the other hand, ultrasonic signature analysis can satisfy all three of the requirements and thus possess a greater potential of success in the field of non-destructive testing.

D. Description of the Overall Project.

1. Principle of ultrasonic signature analysis.

The source of ultra-sound is a piezoelectric transducer. The transmitting transducer is excited to send an ultrasonic signal into the specimen under test. The output signal is detected by the receiving transducer located at a strategic position. The receiving transducer can produce a complex electric signal which serves as the signature, in response to the ultra-sound. Small changes in structure, such as crack formation, work hardening, plastic deformation, etc., will correspond to changes in ultrasonic signature. The changes are extremely sensitive to the size of the defects. By analyzing the signature, one can determine the location and size of the defect.

2. Project Phases

The project can be divided into the following phases:

a. Phase I - Simple specimen, simulated defect.

b. Phase II - Simple specimen, defect produced by fatigue loading.

c. Phase III - Small scale model.

d. Phase IV - Full scale model.

3. Block diagram

The system used to obtain ultrasonic signature is described in a block diagram (see Fig. 1.)

E. Description of the Phase I.

The object of this thesis is to investigate the theoretical background of ultrasonic signature analysis and this theoretical work is corresponding to the phase I of the overall project.

The experiment with simple specimen and simulated defect will be completed later. The proposed experimental model is shown in Fig. 2.

The structure is represented by a rectangular aluminum plate and the flaw is simulated by a drilled cylindrical hole of radius r_o located in a sufficiently large distance from the source. An ultrasonic pulse, generated by the transmitting transducer, is sent into the specimen. The output pulse is detected by a receiving transducer. However, due to attenuation, the receiving pulse may have such a low amplitude that it is buried under the noise. If we cross correlate the transmitting and receiving pulses, noise can be eliminated (See next section). This method is made possible by the appearance of the Fast Fourier Analyzer in the commerical market recently.

F. Cross-correlation Technique in Noise Elimination.

A periodic signal masked by noise can be detected by cross-correlation technique in time domain. If the same technique is done in frequency domain, it is called filtering. [10].

Let us consider the cross-correlation $\phi_{SR}(t)$ between input signal $f_1(t)$ and output signal $f_2(t)$ which is masked by noise $n(t)$. We assume the following conditions:

1. Signals are periodic.
2. The input signal $f_1(t)$ is noise free.
3. The noise is white and at random.
4. There is no cross-correlation between periodic signal and random noise.

Let

$$S(t) = f_1(t)$$

$$R(t) = f_2(t) + n(t)$$

The cross-correlation between S(t) and R(t) is defined as:

$$\phi_{SR}(t) = \lim_{T_o \to \infty} \frac{1}{T_o} \int_{-T_o/2}^{T_o/2} S(t)\, R(t - \tau)dt$$

where

T_o is period and $R(t - \tau)$ is the output signal R(t) delayed by a time constant τ.

$$R(t - \tau) = f_2(t - \tau) + n(t - \tau)$$

then

$$\phi_{SR}(t) = \lim_{T_o \to \infty} \frac{1}{T_o} \int_{-T_o/2}^{T_o/2} f_1(t) \left[f_2(t - \tau) + n(t - \tau) \right] dt$$

$$= \lim_{T_o \to \infty} \frac{1}{T_o} \int_{-T_o/2}^{T_o/2} f_1(t)\, f_2(t - \tau)dt + \lim_{T_o \to \infty} \frac{1}{T_o} \int_{-T_o/2}^{T_o/2} f_1(t)\, n(t - \tau)dt$$

$$= \phi_{12}(\tau) + \phi_{1n}(\tau)$$

since we assume that there is no correlation between periodic signal $f_1(t)$ and random noise n(t)

$$\phi_{1n}(\tau) = o$$

therefore

$$\phi_{SR}(\tau) = \phi_{12}(\tau).$$

Notice that the final expression of $\phi_{SR}(\tau)$ is noise free. It is im portant to point out that the definition of cross-correlation depends on how the time shift constant τ is being defined. The definition of τ is shown in the next section.

II CROSS-CORRELATION FUNCTION AND CROSS POWER SPECTRUM OF A TRANSMITTING SIGNAL AND RECEIVING SIGNAL

A. General Description.

A transmitting pulse S(t) of pulse height p_o is sent into the specimen, and the receiving pulse R(t) with pulse height of ηp_o, where η is the constant factor due to attenuation, is detected. The transit time between S(t) and R(t) is T_R. The pulse width for both pulses is a and the repetition rate (period) is T_o. The diagram of the pulses vs. time is shown in Fig. 3.

B. Cross-correlation of S(t) and R(t).

The cross-correlation of two periodic function, S(t) and R(t), is found by taking one of the signals, multiplying by another signal, displaced τ unit of time, and averaging over all time.

$$\phi_{SR}(\tau) = \frac{1}{T_o} \int_{-T_{o/2}}^{T_{o/2}} S(t)\, R(t - \tau)dt$$

In order to simplify the problem, let us assume that S(t) is held in a fixed position and R(t) is allowed to displaced from left to right. The two functions, then, can be cross correlated in two separated region, I and II.

1. Region I.

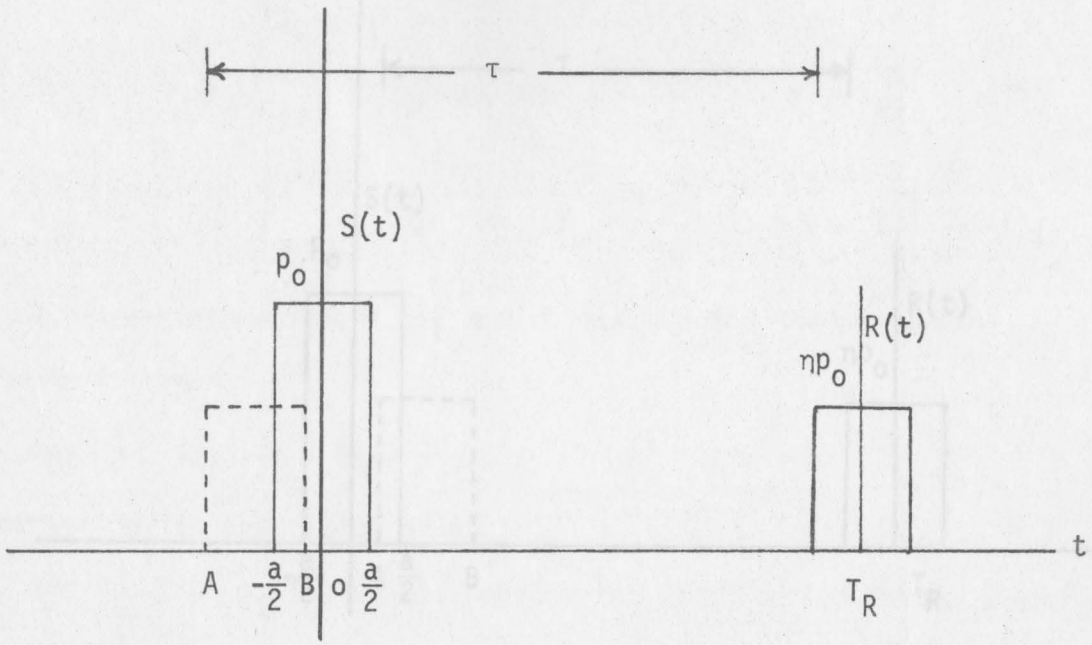

Fig. A. Cross-correlation between R(t) and S(t) in region I

In this region, the correlation starts when the receiving pulse edge B enters the fixed S(t) and ends when the receiving pulse is directly on top of S(t), as R(t) is allowed to sweep from left to right. The limits of integration in this region are:

$$-\frac{a}{2} < t < \frac{a}{2} - \tau + T_R$$

$$T_R < \tau < T_R + a$$

The cross-correlation function in Region I, $\phi_{SR}(\tau)_I$, is

$$\phi_{SR}(\tau)_I = \frac{1}{T_o}\int_{-a/2}^{a-\tau+T_R} S(t)\, R(t-\tau)dt$$

2. Region II.

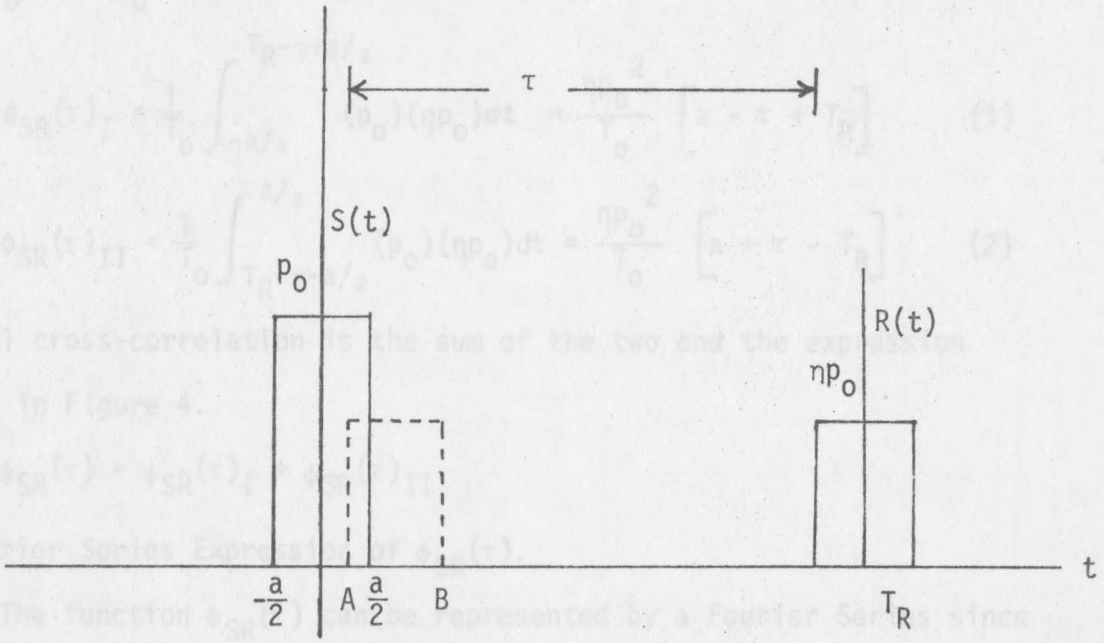

Fig. B. Cross-correlation between S(t) and R(t) in region II

In this region, the cross-correlation starts when receiving pulse is directly on top of the transmitting pulse and ends when the receiving pulse moves completely out of the transmitting pulse, as R(t) is allowed to sweep over the fixed S(t) from left to right. The limit of integration in this region are

$$\frac{a}{2} < t < T_R - \tau - \frac{a}{2}$$

$$T_R < \tau < T_R - a$$

The cross-correlation function in region II, $\phi_{SR}(\tau)_{II}$, is

$$\phi_{SR}(\tau)_{II} = \frac{1}{T_o}\int_{T_R-\tau-a/2}^{a/2} S(t)\, R(t-\tau)dt$$

Since the transmitting pulse and the receiving pulse has pulse height p_o and ηp_o respectively, therefore,

$$\phi_{SR}(\tau)_I = \frac{1}{T_o}\int_{-a/2}^{T_R-\tau+a/2} (p_o)(\eta p_o)dt = \frac{\eta p_o^2}{T_o}\left[a - \tau + T_R\right] \qquad (1)$$

$$\phi_{SR}(\tau)_{II} = \frac{1}{T_o}\int_{T_R-\tau-a/2}^{a/2} (p_o)(\eta p_o)dt = \frac{\eta p_o^2}{T_o}\left[a + \tau - T_R\right] \qquad (2)$$

The total cross-correlation is the sum of the two and the expression is shown in Figure 4.

$$\phi_{SR}(\tau) = \phi_{SR}(\tau)_I + \phi_{SR}(\tau)_{II}$$

C. Fourier Series Expression of $\phi_{SR}(\tau)$.

The function $\phi_{SR}(\tau)$ can be represented by a Fourier Series since it is periodic.

$$\phi_{SR}(\tau) = \sum_{n=-\infty}^{\infty} C_n e^{in\omega_o t} \qquad (3)$$

$$C_n = \frac{1}{T_o}\int_{T_o} \phi_{SR}(\tau)e^{-in\omega_o\tau}\, d\tau \qquad n = o, 1, 2, ...$$

where

$$\omega_o = 2\pi f_o = \frac{2\pi}{T_o}$$

Substitute (1) and (2) into the expression of C_n

$$C_n = \underbrace{\frac{1}{T_o}\int_{T_R+a}^{T_R} \phi_{SR}(\tau)_I\, e^{-i2\pi nf_o\tau}\, d\tau}_{I_1} + \underbrace{\frac{1}{T_o}\int_{T_R}^{T_R-a} \phi_{SR}(\tau)_{II}\, e^{-i2\pi nf_o\tau}\, d\tau}_{I_2}$$

1. Integral I.

$$I_1 = \frac{1}{T_o}\int_{T_R+a}^{T_R} \phi_{SR}(\tau)_I \, e^{-i2\pi n f_o \tau} \, d\tau$$

$$= \frac{1}{T_o}\int_{T_R+a}^{T_R} \frac{\eta p_o^2}{T_o} \left[a - \tau + T_R\right] e^{-i2\pi n f_o \tau} \, d\tau$$

$$= \frac{\eta p_o^2}{T_o}\left[(a + T_R)\int_{T_R+a}^{T_R} e^{-i2\pi n f_o \tau} \, d\tau - \int_{T_R+a}^{T_R} \tau e^{-i2\pi n f_o \tau} \, d\tau \right]$$

$$= \frac{\eta p_o^2}{T_o}\left\{ \left[(a + T_R)\left(\frac{e^{-i2\pi n f_o \tau}}{-i2\pi n f_o}\right)\right] - \left[\frac{e^{-i2\pi n f_o \tau}}{-i2\pi n f_o}\left(\tau + \frac{1}{i2\pi n f_o}\right)\right]\right\}\Bigg|_{T_R+a}^{T_R}$$

After substitution of the limit and simplification,

$$I_1 = \frac{\eta p_o^2 \, e^{-i2\pi n f_o T_R}}{T_o^2 \, (-i2\pi n f_o)}\left[a - \frac{1}{i2\pi n f_o} + \frac{e^{-i2\pi n f_o a}}{i2\pi n f_o}\right]$$

2. Integral I_2.

$$I_2 = \frac{1}{T_o}\int_{T_R}^{T_R-a} \phi_{SR}(\tau)_{II} \, d\tau$$

$$= \frac{1}{T_o}\int_{T_R}^{T_R-a} \frac{\eta p_o^2}{T_o}\left[a + \tau - T_R\right] d\tau$$

$$= \frac{\eta p_o^2}{T_o^2}\left\{ (a - T_R)\left[\frac{e^{-i2\pi n f_o \tau}}{-i2\pi n f_o}\right] + \left[\frac{e^{-i2\pi n f_o \tau}}{-i2\pi n f_o}\left(\tau + \frac{1}{i2\pi n f_o}\right)\right]\right\}\Bigg|_{T_R}^{T_R-a}$$

After substitution of the limits and simplification

$$I_2 = \frac{\eta p_o^2 e^{-i2\pi n f_o T_R}}{T_o^2 (-i2\pi n f_o)} \left[-a + \frac{e^{i2\pi n f_o a} - 1}{i2\pi n f_o} \right]$$

Since $C_n = I_1 + I_2$

after simplification

$$C_n = \frac{\eta p_o^2 a^2}{T_o^2} e^{-i2\pi n f_o T_R} \left[\frac{\mathrm{Sin}(n\pi f_o a)}{(n\pi f_o a)} \right]^2$$

using $\mathrm{Sinc}\ u = \frac{\mathrm{Sin}\ \pi u}{\pi u}$

$$C_n = \frac{\eta p_o^2 a^2}{T_o^2} e^{-i2\pi n f_o T_R} \left[\mathrm{sinc}(n f_o a) \right]^2 \qquad (4)$$

D. Cross Power Spectrum $G_{SR}(f)$

The cross power spectrum $G_{SR}(f)$ is defined as the Fourier transform of the Fourier Series $\phi_{SR}(\tau)$.

$$G_{SR}(f) = \int_{-\infty}^{\infty} \phi_{SR}(\tau)\, e^{-i2\pi f t}\, dt$$

$$= \int_{-\infty}^{\infty} \left(\sum_{n=-\infty}^{\infty} C_n e^{i2\pi n f_o t} \right) e^{-i2\pi f t}\, dt$$

$$= \sum_{n=-\infty}^{\infty} C_n \int_{-\infty}^{\infty} e^{-i(2\pi f - 2\pi n f_o)t}\, dt$$

and $\int_{-\infty}^{\infty} e^{-i(2\pi f - 2\pi n f_o)t}\, dt = \delta(f - n f_o)$

is defined as the impulse function (See Appendix A) so, after substitution

$$G_{SR}(f) = \sum_{n=-\infty}^{\infty} C_n \quad \delta(f - nf_o) \tag{5}$$

substitute (4) in (5)

$$G_{SR}(f) = \frac{\eta p_o^2 a^2}{T_o^2} \sum_{n=-\infty}^{\infty} e^{-i2\pi n f_o T_R} \left[\text{Sinc } nf_o a\right]^2 \delta(f - nf_o) \tag{6}$$

It is important to know that cross power spectrum can be defined as

$$G_{SR}(f) = \underline{S}(f) \times \underline{R}^*(f)$$

where

$\underline{S}(f)$ and $\underline{R}(f)$ are the Fourier transform of $S(t)$ and $R(t)$ repectively, and $\underline{R}^*(f)$ is the complex conjudgate of $R(f)$.

However, this method will lead to the same result. The factor η is the attenuation constant. Attenuation is caused by the scattering of incident sound wave from the cylindrical hole. The scattering effect and attenuation constant η are described in the next section.

III SOUND WAVE SCATTERED FROM A CYLINDRICAL HOLE

A. Description of scattering phenomena [11].

When a travelling plane wave strikes an obstacle along its path in a medium, scattering phenomena occur. The behavior of the scattered wave depends on the dimension of the wavelength relative to the size of the obstacle. In case of ultra-sound, the wavelength is very short compared to the radius of the cylinder, then half of the scattered wave spreads out in all directions and the other half is concentrated behind the obstacle, interfering destructively with the unchanged plane wave behind the obstacle to create a sharp-edged shadow. The case that the ultrasonic wave scattered by the cylindrical hole is analogous to the case of electromagnetic wave whose polarization having the electric

intensity parallel to the axis of the cylinder with perfect conduction. Before the problem can be analyzed, the boundary conditions and several assumptions must be examined.

B. Assumptions and Boundary Conditions.

1. Assumptions.

a. The incident wave is a plane wave.

b. The wave has no dispersion.

c. No shear rigidity - thus no mode conversion.

d. The medium is linear - thus no harmonic generation.

e. Far-field approximation - the distance between the source and the obstacle is very large compared to the radius of the cylindrical hole. ($r >> r_o$)

2. Boundary conditions.

Since the obstacle is a cylindrical hole, the sum of incident wave pressure p_p and the scattered wave pressure p_s must be zero at the surface of the cylinder.

$$p_s + p_p = o \quad \text{at} \quad r = r_o$$

C. Incident and Scattered Wave.

The incident wave p_p is assumed to be a plane wave which is generated from a large distance away. The scattered wave p_s radiates outward from the surface of the cylinder, thus can be expressed by the Hankel functions of the first kind. [12]

$$p_p = p_o e^{ik(r\cos\phi - ct)}$$

$$= p_o \left[J_o(kr) + 2 \sum_{m=1}^{\infty} i^m \cos(m\phi) J_m(kr) \right] e^{-2\pi i f t} \qquad (7)$$

Assume

$$p_s = \sum_{m=o}^{\infty} A_m \cos(m\phi) \left[J_m(kr) + i\, N_m(kr) \right] e^{-2\pi i f t} \qquad (8)$$

$$m = 0, 1, 2, \ldots\ldots$$

where

$k = \frac{2\pi}{\lambda}$

$J_m(kr)$ = Bessel function of m^{th} order with argument kr

$N_m(kr)$ = Neumman function of m^{th} order with argument kr

$H_m(kr) = J_m(kr) + i\, N_m(kr)$ = Hankel function of the 1^{st} kind

A_m = Fourier-Bessel coefficients to be determined

$i = \sqrt{-1}$

$p_o = \sqrt{\rho c I}$ where I is intensity, ρ is mean density and c is wave velocity

we would like to define the phase shift for cylindrical scattering, θ_m

$$J_m(kr_o) = B_m \cos \theta_m$$

$$N_m(kr_o) = B_m \sin \theta_m \qquad [13] \qquad (9)$$

then

$$\tan \theta_m = \frac{N_m(kr_o)}{J_m(kr_o)}$$

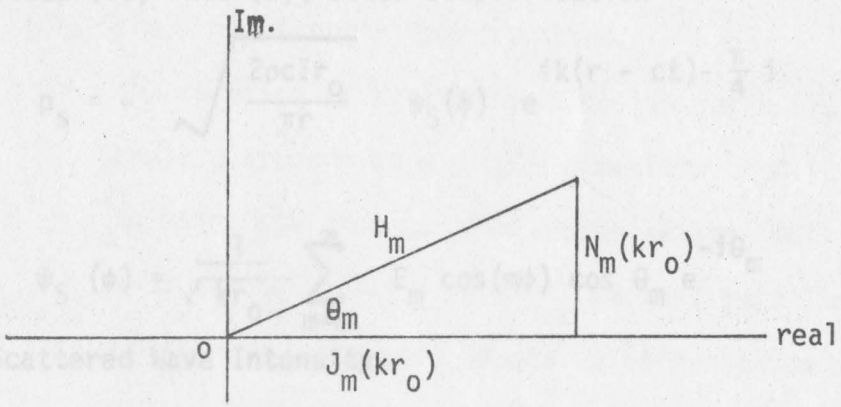

Figure C Definition of phase shift angle θ_m

By applying the boundary conditions to equation (7) and (8) at the surface of the cylinder yields

$$p_p(r = r_o) = \left\{ p_o\, J_o(kr_o) + 2 \sum_{m=1}^{\infty} p_o\, i^m \cos(m\phi)\, J_m(kr_o) \right\} e^{-2\pi i f t} \qquad (10)$$

$$p_s(r = r_o) = \left\{ A_o \left[J_o(kr_o) + i\, N_o(kr_o) \right] + \sum_{m=1}^{\infty} A_m \cos(m\phi) \left[J_m(kr_o) + i\, N_m(kr_o) \right] \right\} e^{-2\pi i f t}$$

since

$$p_s = - p_p \qquad \text{at } r = r_o \tag{11}$$

The two equations (10) and (11) can be matched at the boundary using

$$J_m(kr_o) + i\, N_m(kr_o) = \sqrt{\frac{2}{\pi kr_o}}\, e^{i\left[kr_o - \frac{\pi}{4}(2m+1)\right]} \qquad \text{for large } kr_o \tag{12}$$

The constant A_m is thus found to be

$$A_m = - E_m i^m p_o e^{-i\theta_m} \cos\theta_m \tag{13}$$

where

E_m is defined by Morse [14] as

$$E_m = \begin{cases} 1 & \text{for } m = o \\ 2 & \text{for } m > o \end{cases}$$

Substitute (13) into (8), after simplification

$$p_s = - \sqrt{\frac{2\rho c I r_o}{\pi r}}\, \psi_S(\phi)\, e^{ik(r - ct) - \frac{\pi}{4} i} \tag{14}$$

where

$$\psi_S(\phi) = \frac{1}{\sqrt{kr_o}} \sum_{m=o}^{\infty} E_m \cos(m\phi) \cos\theta_m\, e^{-i\theta_m} \tag{15}$$

D. Scattered Wave Intensity.

It is important to study the intensity of the scattered wave and how it is altered by the change in dimension of the cylindrical hole. The ratio of scattered intensity $S(\phi)$ is defined as

$$S(\phi) = \frac{r_o}{\pi r} \left| \psi_s(\phi) \right|^2$$

$$= \frac{r_o}{\pi r} \left[\psi_s(\phi) \times \psi_s^*(\phi) \right] \qquad (16)$$

where $\psi_s^*(\phi)$ is the complex conjudgate of $\psi_s(\phi)$

using (15) and (16)

$$\left| \psi_s(\phi) \right|^2 = \left[\frac{1}{\sqrt{kr_o}} \sum_{m=o}^{\infty} E_m \cos(m\phi) \cos\theta_m e^{-i\theta_m} \right] \times \left[\frac{1}{\sqrt{kr_o}} \sum_{n=o}^{\infty} E_n \cos(n\phi) \cos\theta_n e^{i\theta_n} \right]$$

$$\left| \psi_s(\phi) \right|^2 = \frac{1}{kr_o} \sum_{m=o}^{\infty} \sum_{n=o}^{\infty} E_m E_n \cos\theta_m \cos\theta_n \cos(\theta_n - \theta_n) \cos m\phi \cos n\phi \qquad (17)$$

thus

$$S(\phi) = \frac{1}{\pi kr} \sum_{m=o}^{\infty} \sum_{n=o}^{\infty} E_m E_n \cos\theta_m \cos\theta_n \cos(\theta_m - \theta_n) \cos(m\phi) \cos(n\phi) \qquad (18)$$

1. Short Wave Length Approximation.

The equation of scattered intensity ratio $S(\phi)$ vs. scattered angle ϕ appears as a double summation, and it is so difficult to calculate that certain approximations will have to be made in order to obtain simpler expressions. Since ultra-sound has a very short wave length relative to the size of the hole, we can investigate the short wave length approximation. Let us consider the asymptotic value of θ_m for short wavelength, that is, $kr_o \gg 1$. Equation (12) can be written as

$$J_m(kr_o) + i\, N_m(kr_o) = \sqrt{\frac{2}{\pi kr_o}} \left[\cos\left(kr_o - \frac{\pi}{4}(2m+1)\right) + i \sin\left(kr_o - \frac{\pi}{4}(2m+1)\right) \right] \qquad (19)$$

comparing (19) and (9)

$$\theta_m = kr_o - \frac{\pi}{4}(2m + 1) \qquad (20)$$

substitute (20) into (18), after necessary mathematical manipulations are made, the scattered intensity ratio is found to be [15] (See appendix c)

$$S(\phi) = \frac{r_o}{2r}\sin(\phi/2) + \frac{1}{2\pi kr}\cot^2(\phi/2)\sin^2(kr_o\phi) \qquad (21)$$

it is important to know that for very short wavelength, the scattered intensity only appears as an average and the average intensity varies smoothly per degree [16].

2) Far-field radiation pattern of scattered intensity $|\psi_s(\phi)|^2$ vs. scattered angle ϕ for different sizes of hole.

The far-field radiation patterns of several different sizes of hole are shown in Fig. 5. For $\lambda \simeq r_o$, the graphs were plotted using equation (18), and for $\lambda << r_o$, the graphs were plotted using equation (21). It is important to know that the scattered wave intensity cannot be measured for $\phi = o$ or $\phi = \pi$, exactly in the direction of plane wave or opposite to it. If the graph varies smoothly for ϕ very close to o or π, the intensity can be extrapolated with fairly accurate result. The first term in (21) represents the reflected intensity and the second term is the shadow-forming wave because it has a very high peak in the region $\phi \simeq o$ which is corresponding to the direction of the plane wave, therefore, tends cancelling it to form a shadow. [17] By observing the radiation patterns, we can see that a small change in dimension of the hole will change the scattered

intensity significantly. This is essential to our analysis because it leads to the conclusion that the radiation pattern is very sensitive to the size of the defect.

E. Change of Sound Wave Pressure Due to Scattering.

Since the piezoelectric transducer, which is used to detect the receiving sound pulses cannot distinguish the difference between the incident and scattered wave, we have to focus our attention on the investigation of the average pressure at the surface of the receiving transducer.

Recall equation (7) and (14), the incident and scattered wave can be written as

$$p_p = p_o\, e^{-i\omega t} \sum_{m=o}^{\infty} E_m\, i^m\, J_m(kr)\, \cos(m\phi) \tag{22}$$

$$p_s = -\sqrt{\frac{2\rho c I r_o}{\pi r}}\, \frac{1}{\sqrt{kr_o}}\, e^{ik(r-ct)-\frac{\pi}{4}i} \sum_{m=o}^{\infty} E_m \cos(m\phi)\, \cos\theta_m e^{i\theta_m} \tag{23}$$

using the relationship

$$i^m = e^{\frac{im\pi}{2}}$$

and making far field approximation, (22) and (23) becomes

$$p_p = p_o \sqrt{\frac{1}{2\pi ikr}} \left\{ e^{ikr} \sum_{m=o}^{\infty} E_m \cos(m\phi) + i\, e^{ikr} \sum_{m=o}^{\infty} E_m \cos\Big(m(\phi-\pi) \Big) \right\} e^{-i\omega t} \tag{24}$$

$$p_s = -\, p_o \sqrt{\frac{2}{\pi kr}} \sum_{m=o}^{\infty} E_m e^{-i\left(\theta_m + \frac{\pi}{4}\right)} \cos\theta_m \cos(m\phi)\, e^{ikr} \tag{25}$$

The total wave that reaches the receiving transducer is

$$p_s + p_p = p_o \sqrt{\frac{1}{2\pi ikr}} \left\{ \underbrace{i\, e^{-ikr-i\omega t} \sum_{m=o}^{\infty} E_m \left[\cos\ m(\phi-\pi)\right]}_{(I)} + \underbrace{e^{ikr-i\omega t} \sum_{m=o}^{\infty} E_m\, e^{-2i\left[\theta_m(kr_o) + \frac{\pi}{2}\right]} \cos(m\phi)}_{(II)} \right\} \qquad (26)$$

Let us consider some important relationships

1) asymptotic value of θ_m for short wavelength

$$\theta_m = kr_o - \frac{\pi}{4}(2m+1)$$

2) $$e^{-2i(\theta_m(kr_o) + \frac{\pi}{2})} = e^{-2i\left[kr_o - \frac{m\pi}{2} + \frac{\pi}{4}\right]}$$

$$= \frac{1}{i}\, e^{-2ikr_o}$$

3) $$\sum_{m=o}^{M} E_m \cos(\phi-\pi) = \lim_{m\to kr_o} \frac{\mathrm{Sin}(M + \frac{1}{2})(\phi-\pi)}{\mathrm{Sin}\ \frac{1}{2}(\phi-\pi)} \qquad [18]$$

using these relationship, the first term of equation (26) is

$$(I) = -\frac{p_o}{i}\sqrt{\frac{1}{2\pi ikr}}\ e^{-ikr}\ \frac{\sin\left[(kr_o + \frac{1}{2})(\phi-\pi)\right]}{\sin\frac{1}{2}(\phi-\pi)}$$

The second term of (26) is

$$(II) = \frac{p_o}{i}\sqrt{\frac{1}{2\pi ikr}}\ e^{ikr}\ e^{-2ikr_o}\ \frac{\sin\left[(kr_o + \frac{1}{2})(\phi-\pi)\right]}{\sin\frac{1}{2}(\phi-\pi)}$$

The asymptotic value of total pressure wave p_T is the sum of (I) and (II)

$$p_T = p_p + p_s = \frac{p_o}{i}\sqrt{\frac{1}{2\pi ikr}}\left[e^{ikr}\, e^{-2ikr_o} + e^{-ikr}\right] \frac{\sin\left[(kr_o + \frac{1}{2})(\phi-\pi)\right]}{\sin\frac{1}{2}(\phi-\pi)}$$

after simplification, the expression becomes

$$p_T = p_o \sqrt{\frac{2}{i\pi kr}}\, e^{-ikr_o} \sin k(r-r_o)\, \frac{\sin\left[(kr_o + \frac{1}{2})(\phi-\pi)\right]}{\sin \frac{1}{2}(\phi-\pi)} \qquad (27)$$

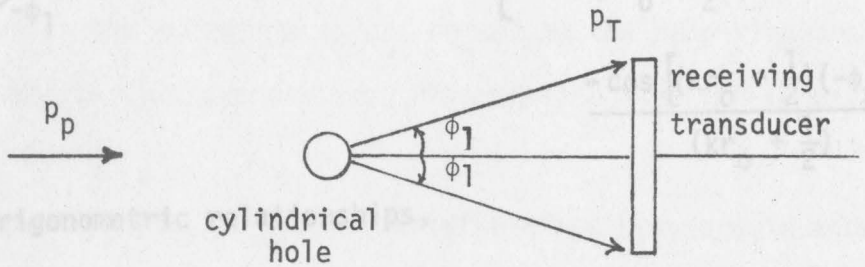

Figure D Average pressure $<p_T>$ senses by the receiving transducer over small angle ϕ_1

The average pressure $<p_T>$ sense by the receiving transducer over a small angle ϕ_1 is

$$<p_T> = \frac{1}{2\phi_1} \int_{-\phi_1}^{\phi_1} p_o \sqrt{\frac{2}{\pi ikr}}\, \sin k(r-r_o)\, \frac{\sin\left[(kr_o + \frac{1}{2})(\phi-\pi)\right]}{\sin \frac{1}{2}(\phi-\pi)}\, d\phi \qquad (28)$$

but the angle ϕ_1 and radius r_o are very small comparing to π and r respectively, we can assume that

$$\sin k(r - r_o) \eqsim \sin kr$$

and

$$\sin \frac{1}{2}(\phi-\pi) \approx \sin \frac{1}{2}(-\pi) \approx -1$$

then (28) becomes

$$\langle p_T \rangle = \frac{p_o}{2\phi_1}\sqrt{\frac{2}{\pi i k r}}\,\sin kr \int_{-\phi_1}^{\phi_1} \sin\left[\left(kr_o + \tfrac{1}{2}\right)(\phi-\pi)\right]\, d\phi \qquad (29)$$

consider the integral

$$\int_{-\phi_1}^{\phi_1} \sin\left[\left(kr_o + \tfrac{1}{2}\right)(\phi-\pi)\right]\, d\phi = -\left[\frac{\cos\left[\left(kr_o + \tfrac{1}{2}\right)(\phi_1-\pi)\right]}{\left(kr_o + \tfrac{1}{2}\right)} + \frac{-\cos\left[\left(kr_o + \tfrac{1}{2}\right)(-\phi_1-\pi)\right]}{\left(kr_o + \tfrac{1}{2}\right)}\right]$$

using trigonometric relationships,

$$\int_{-\phi_1}^{\phi_1} \sin\left[\left(kr_o + \tfrac{1}{2}\right)(\phi-\pi)\right]\, d\phi = \frac{-2}{\left(kr_o + \tfrac{1}{2}\right)}\left\{\sin\left[\left(kr_o + \tfrac{1}{2}\right)\phi_1\right]\right\} \times \left\{\sin\left[\left(kr_o + \tfrac{1}{2}\right)\pi\right]\right\} \qquad (30)$$

substitute (30) into (29), the average pressure is

$$\langle p_T \rangle = p_o\, \frac{1}{\left(kr_o + \tfrac{1}{2}\right)\phi_1}\sqrt{\frac{2}{\pi i k r}}\,\sin kr\, \sin\left[\left(kr_o + \tfrac{1}{2}\right)\phi_1\right] \times \sin\left[\left(kr_o + \tfrac{1}{2}\right)\pi\right] \qquad (31)$$

IV CROSS POWER SPECTRUM OF TRANSMITTING AND RECEIVING PULSES AFTER SCATTERING FROM A CYLINDRICAL HOLE

The cross power spectrum of the transmitting and receiving pulse is shown in equation (6). The factor η, as we pointed out before, has not yet been determined. Since the amplitude of the receiving pulse is the same as the average pressure sensed by the receiving transducer, we can equate the two expressions. The amplitude of the receiving pulse is

$$R = \eta\, p_o$$

and comparing with the expression of average pressure in equation (31), we know that

$$\eta = \frac{1}{(kr_o + \frac{1}{2})\phi_1}\sqrt{\frac{2}{\pi i k r}}\,\sin(kr)\,\sin\left[(kr_o + \tfrac{1}{2})\phi_1\right]\sin\left[(kr_o + \tfrac{1}{2})\pi\right] \tag{32}$$

The factor η is very sensitive to the size of the defect. The final expression for the cross power spectrum is

$$G_{SR}(f) = \left\{\frac{1}{(kr_o + \frac{1}{2})\phi_1}\sqrt{\frac{2}{\pi i k r}}\,\sin\left[(kr_o + \tfrac{1}{2})\phi_1\right]\,\sin\left[(kr_o + \tfrac{1}{2})\pi\right]\sin(kr)\right.$$
$$\left. x\left\{\frac{P_o{}^2 a^2}{T_o{}^2}\sum_{n=-\infty}^{\infty} e^{-i2\pi n f_o T_R}\left[\text{sinc}\ (nf_o a)\right]^2\,\delta\,(f - nf_o)\right\}\right. \tag{33}$$

Since the equation is a very complicated expression, certain simplification must be made. Consider

1) Since the transit time T_R is fixed because the dimension of the specimen is predetermined, one can only make the period T_o in such a way that the factor T_R/T_o $(T_R f_o)$ is a simple number.

2) After simplification

$$\sqrt{\frac{2}{\pi i k r}} = \left[\frac{\sqrt{2}}{2} - i\,\frac{\sqrt{2}}{2}\right]\sqrt{\frac{2}{\pi k r}} \tag{34}$$

notice the spectrum has been separated into real and imaginary part with equal magnitude. Rather than working with a complex function, we only have to concern ourself with the real part or imaginary part.

3) The factor $\frac{a}{T_o}$ (or $f_o a$) can also be made a simple number. By substituting the desired value of $T_R f_o$, $f_o a$, the expression can be greatly simplified. A set of typical experimental parameters has been choosen, and the expression can be shown in Appendix B.

V CONCLUSIONS

The cross power spectrum of the transmitting and receiving pressure pulses has been determined in this paper. The change of pressure in the receiving pulse was caused by the scattering of sound from a defect, simulated by a drilled cylindrical hole. The shape, amplitude, and sensitivity of the spectrum have been discussed in Appendix B. The success of the Ultrasonic Signature Analysis depends on whether the change in dimension of the defect is detectable. It has been shown that the cross power spectrum is very sensitive to the radius of the cylindrical hole and the changes can be determined by the Fourier Analyzer.

Before using the equation of cross power spectrum, one has to keep in mind that it is developed under certain assumptions. If any changes alter the system in such a way that our assumptions are no longer valid, the expression may become inaccurate. For example, the wavelength of the ultra-sound is assumed to be much shorter than the radius of the hole. If the radius of the hole becomes so small that it is shorter than the wavelength of the ultra-sound, the short wavelength approximation fails. Although a hole of such a size may not be too significant to cause any damage in the complex structure, yet it is recommended that the long wavelength approximation should be considered in the future.

Experiments should be conducted later to see whether it agrees with the theoretical results. The sensitivity of the corresponding changes in the spectrum and the radius of the hole should also be examined.

If the experiment confirms with the theory, further effort should be made to study the small cracks emanating from the hole and different types of defects such as rivets, bolts, fatigue-loading etc. These experiments should eventually lead to the construction of the small scale and full scale model.

APPENDIX A

The impulse function: [19] [20]

A unit impulse (also called Delta function) has a unit area or weight at the point where the argument is zero and the impluse is zero everywhere else. It can be written as

$$\delta(x) = \begin{cases} 0 & x \neq 0 \\ \infty & x = 0 \end{cases}$$

$$\int_{-\infty}^{\infty} \delta(x) = 1$$

for a impulse A $\delta(x)$ with weight A can be represented graphically below

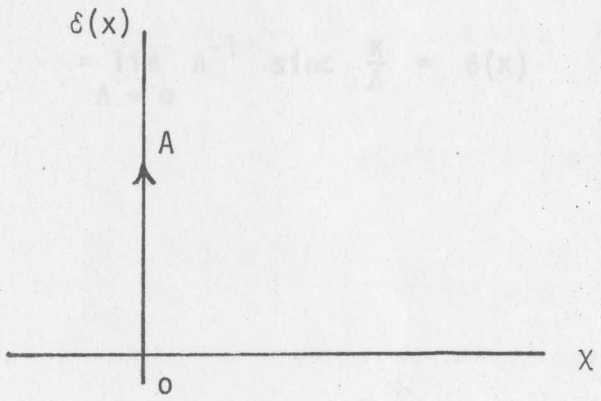

It is important to know that, in strict sense, impulse is not a function. Certain conventional interpretation must be declared, otherwise, the expressions is meaningless.

There are many possible shapes which become impulses in limit, let the duration be Λ, then

$$\delta(x) = \lim_{\Lambda \to o} \begin{cases} \Lambda^{-1} e^{-\pi(\frac{x}{\Lambda})^2} & \text{gassian} \\ \Lambda^{-1} \Pi(\frac{x}{\Lambda}) & \text{rectangular} \\ \Lambda^{-1} \text{Sinc } \frac{x}{\Lambda} & \text{Sinc} \\ \Lambda^{-1} \text{Sinc}^2 \frac{x}{\Lambda} & \text{Sinc}^2 \end{cases}$$

The improper integral used in page 11 can be expressed as impulse function

$$\int_{-\infty}^{\infty} e^{-i2\pi xt} \, dt = \lim_{\Lambda \to o} \int_{-\frac{1}{2\Lambda}}^{\frac{1}{2\Lambda}} e^{-i2\pi xt} \, dt$$

$$= \lim_{\Lambda \to o} \Lambda^{-1} \text{ sinc } \frac{x}{\Lambda} = \delta(x)$$

APPENDIX B

Sample calculation for cross power spectrum

From equation (33) the cross power spectrum can be written as

$$G_{SR}(f) = \left\{ \frac{1}{(kr_o + \frac{1}{2})\phi_1} \sqrt{\frac{2}{\pi i k r}} \sin(kr) \sin\left[(kr_o + \frac{1}{2})\phi_1\right] \sin\left[(kr_o + \frac{1}{2})\pi\right] \right\}$$

$$x \left\{ \frac{p_o^2 a^2}{T_o^2} \sum_{n=-\infty}^{\infty} e^{-i2\pi n f_o T_R} \left[\sin c\ (nf_o a)\right]^2 \delta(f - nf_o) \right\}$$

substitute (34) into (33), the real part of $G_{SR}(f)$ is

$$R_e\left[G_{SR}(f)\right] = \frac{1}{\sqrt{\pi kr}} \times \frac{1}{2\phi_1} \frac{p_o^2 a^2}{T_o^2} \sin kr \times \frac{1}{(kr_o + \frac{1}{2})}$$

$$\sin\left[(kr_o + \frac{1}{2})\phi_1\right] \sin\left[(kr_o + \frac{1}{2})\pi\right]$$

$$x \sum_{n=-\infty}^{\infty} e^{-i2\pi n f_o T_R} \left[\text{sinc}\ (nf_o a)\right]^2 \delta(f - nf_o) \quad (35)$$

to consider a practical case, these experimental values are picked

Pulse width $a = 100\ \mu\text{sec}$

Transit time $T_R = 100\ \mu\text{sec}$

Period $T_o = 200\ \mu\text{sec}$

so

$$f_o a = \frac{1}{2}$$

$$f_o T_R = \frac{1}{2}$$

$$e^{-i2\pi n f_o T_R} = \cos n\pi$$

substitute these values in (32) and (33)

$$G_{SR}(f) = C_1 \sum_{n=-\infty}^{\infty} (\cos n\pi) \left[\text{sinc}\, nf_o a\right]^2 \delta(f - nf_o) \qquad (36)$$

where

$$C_1 = \frac{\eta p_o^2 a^2}{T_o^2}$$

1. The shape of cross power spectrum.

   Since C_1 appears only as a scale factor, varing with different size of the hole, it does not change the shape of the spectrum. The graph of $G_{SR}(f)$ vs. f is plotted below with the aid of digital computer.

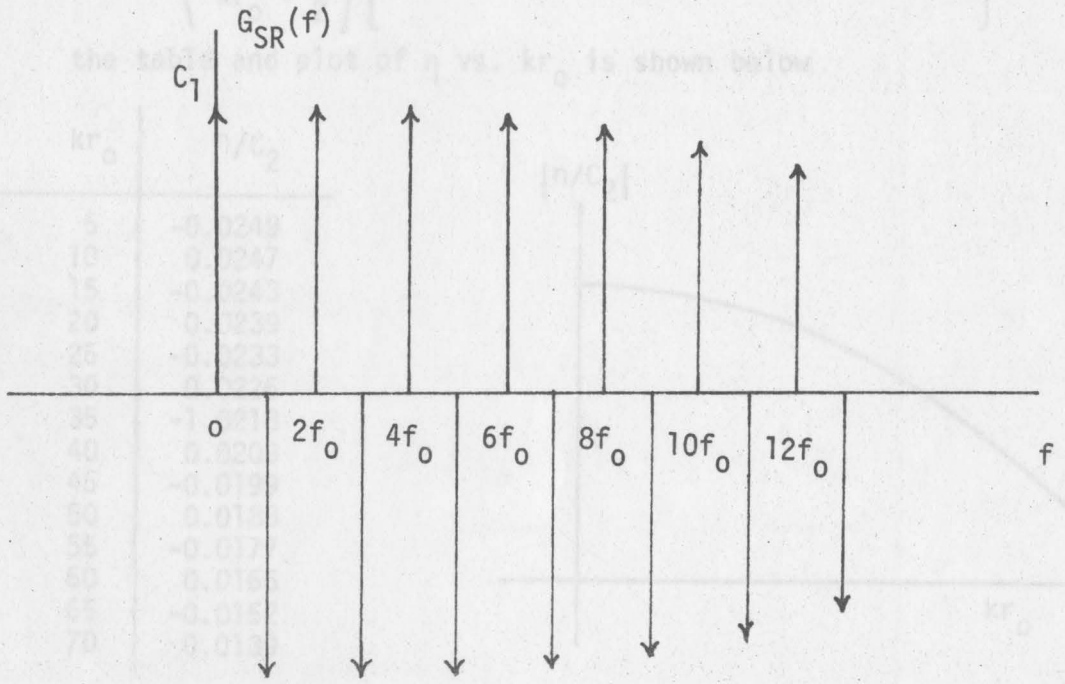

Figure E Cross power spectrum $G_{SR}(f)$ vs. frequency f

2. The magnitude of cross power spectrum with different size of defect.

$$C_1 = \left(\frac{p_o^2 a^2}{T_o^2} \right) \eta$$

Since the factor $\frac{p_o^2 a^2}{T_o^2}$ remains the same for all size of the hole, we only have to consider the factor η from equation (35)

$$\eta = \left(\frac{1}{\sqrt{\pi kr}} \frac{1}{\phi_1} \sin kr\right)\left(\frac{1}{kr_o + \frac{1}{2}}\right) \sin\left[(kr_o + \tfrac{1}{2})\phi_1\right] \sin\left[(kr_o + \tfrac{1}{2})\pi\right] \quad (37)$$

The only variable in this equation is r_o where all the remaining parameters are constant. Equation (37) becomes

$$\eta = C_2\left(\frac{1}{kr_o + \frac{1}{2}}\right)\left\{\sin\left[(kr_o + \tfrac{1}{2})\phi_1\right] \sin\left[(kr_o + \tfrac{1}{2})\pi\right]\right\}$$

the table and plot of η vs. kr_o is shown below

kr_o	η/C_2
5	-0.0249
10	0.0247
15	-0.0243
20	0.0239
25	-0.0233
30	0.0226
35	-1.0218
40	0.0209
45	-0.0199
50	0.0188
55	-0.0177
60	0.0165
65	-0.0152
70	0.0139

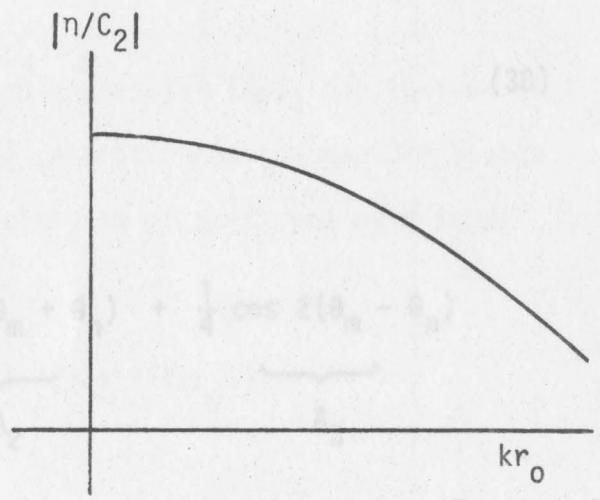

It is important to point out that the changes in η for different kr_o are large enough to be detected by the Fourier Analyzer, which can detect changes in the order of $1 : 10^4$.

APPENDIX C

Mathematical development of $S(\phi)$ in short wavelength approximation.

From equation (18), the scattered wave intensity $S(\phi)$ is found to be

$$S(\phi) = \frac{1}{\pi kr} \sum_{m=o}^{kr_o} \sum_{n=o}^{kr_o} E_m E_n \cos\ \theta_m \cos\theta_n \cos(\theta_m - \theta_n) \cos m\phi \cos n\phi$$

notice the upper limits of the summation have been changed to kr_o because the values of θ_m and θ_n are 0 for $m > kr_o$.

The short wavelength approximation for θ_m is expressed in equation (20) as

$$\theta_m = kr_o - \frac{\pi}{4}(2m + 1)$$

thus

$$\theta_m - \theta_n = -\frac{\pi}{2}(m - n) \qquad (38)$$

using trigonometric indentities,

$$\cos\theta_m \cos\theta_n \cos(\theta_m - \theta_n)$$

$$= \underbrace{\frac{1}{2}\cos^2(\theta_m - \theta_n)}_{A_1} + \underbrace{\frac{1}{4}\cos 2(\theta_m + \theta_n)}_{A_2} + \underbrace{\frac{1}{4}\cos 2(\theta_m - \theta_n)}_{A_3}$$

substitute A_1 into $S(\phi)$ to obtain $S(\phi)_1$

$$S(\phi)_1 = \frac{1}{2\pi kr} \sum_{m=o}^{kr_o} \sum_{n=o}^{kr_o} E_m E_n \cos m\phi \cos n\phi - \frac{1}{2\pi kr} \sum_{m=o}^{kr_o} \sum_{n=o}^{kr_o} E_m E_n \sin^2(\theta_m - \theta_n) \cos m\phi \cos n\phi \qquad (39)$$

using approximation given in page 19,

$$\sum_{m=o}^{kr_o} E_m \cos m\phi = \frac{\sin\left[(kr_o + \frac{1}{2})\phi\right]}{\sin \frac{1}{2}\phi}$$

$S(\phi)_{11}$, the first term of equation (39) is

$$S(\phi)_{11} = \frac{1}{2\pi kr} \sum_{m=o}^{kr_o} E_m \cos m\phi \sum_{n=o}^{kr_o} E_n \cos n\phi$$

$$= \frac{1}{2\pi kr} \left\{ \frac{\sin^2\left[(kr_o + \frac{1}{2})\phi\right]}{\sin^2 \frac{1}{2}\phi} \right\}$$

after simplification

$$S(\phi)_{11} = \frac{1}{2\pi kr} \left[\cot^2 \tfrac{1}{2}\phi \sin^2 kr_o\phi + \sin 2kr_o\phi \cot \tfrac{1}{2}\phi + \cos^2 kr_o\phi \right]$$

After substitution of A_2, A_3 into expression $S(\phi)$, application of short wavelength approximation of θ_m and separation of the rapidly fluctuating terms, the short wavelength approximation of scattered wave intensity can be expressed as

$$S(\phi) = \frac{r_o}{2r} \sin(\phi/2) + \frac{1}{2\pi kr} \cot^2(\phi/2) \sin^2(kr_o\phi)$$

REFERENCES

[1] L. Feinstein and R. Hrwby, "Surface-Crack Detection by Microwave Methods," a paper presented at Sixth Symposium on non-destructive Evaluation of Aerospace and Weapons System Components and Materials," San Antonio, Texas, 17-19 April, 1907

[2] R. S. Sharpe, ed., Research Techniques in Nondestructive Testing, Academic Press, London, 1970

a. R. Halmshaw, "Direct view Radiological Systems."
b. D. W. Lawson and J. W. Sabey, "Infrared Techniques."
c. H. L. Libby, "Multiparameter Eddy Current Concepts."
d. O. R. Gericke, "Ultrasonic Spectroscopy."
e. J. E. Jacobs, "Ultrasonic Imaging System."
f. F. L. Baker and R. L. Richardson, "Ultrasonic Critical Angle Reflectivity."
g. E. E. Addridge, "Ultrasonic Holography."

[3] D. M. Robinson, "Minutes of ad hoc Committee Meeting on Fatigue and Crack Detection," June 25, 1971, NASA-Langley Research Center.

[4] R. J. Exid, ibid.

[5] J. R. Barton, "Magnetic Perturbation Inspection to Improve Reliability of High Strength Steel Components," a paper presented at Design Engineering Conference of ASME, May 5-8, 1968, New York.

[6] J. Langford and P. H. Francis, "Magnetic Field Perturbation Due to Metallurgical Defects." a paper presented at Symposium on Advanced Experimental Technique in the Mechanics of Materials, Sept. 9-11, 1970, San Antonio, Texas.

[7] W. T. Kaarlela, "Magnetic Rubber Inspection," General Dynamics FZM-12-10769

[8] H. L. Dunegan and A. S. Telelman, "Acoustic Emission," Research/ Development, May, 1971

[9] H. A. Cole, Jr., NASA TM x-62, 041

[10] B. P. Lathi, Signals, Systems, and Communication, John Wiley and Sons, Inc., New York, 1965, pp 528-531

[11] P. M. Morse and K. U. Ingard, Theoretical Physics, McGraw-Hill, New York, 1968, pp 400-405

[12] ibid, pp 400-405.

[13] ibid, pp 400-405.

[14] ibid, pp 400-405

[15] P. M. Morse and H. Feshbach, Method of Theoretical Physics, McGraw-Hill, New York, 1953, pp 1380-1381

[16] ibid, pp 1380-1381

[17] P. M. Morse and H. Feshbach, Method of Theoretical Physics, McGraw-Hill, New York, 1953, pp 1377-1378

[18] P. M. Morse and H. Feshbach, Method of Theoretical Physics, McGraw-Hill, New York, 1953, p 1379

[19] R. M. Bracewell, The Fourier Transform and Its Applications, McGraw-Hill, New York, 1965, pp 69-80

[20] A. B. Carlson, Communication Systems: An Introduction to Signals and Noise in Electrical Communication, McGraw-Hill, New York, 1968, pp 45-47

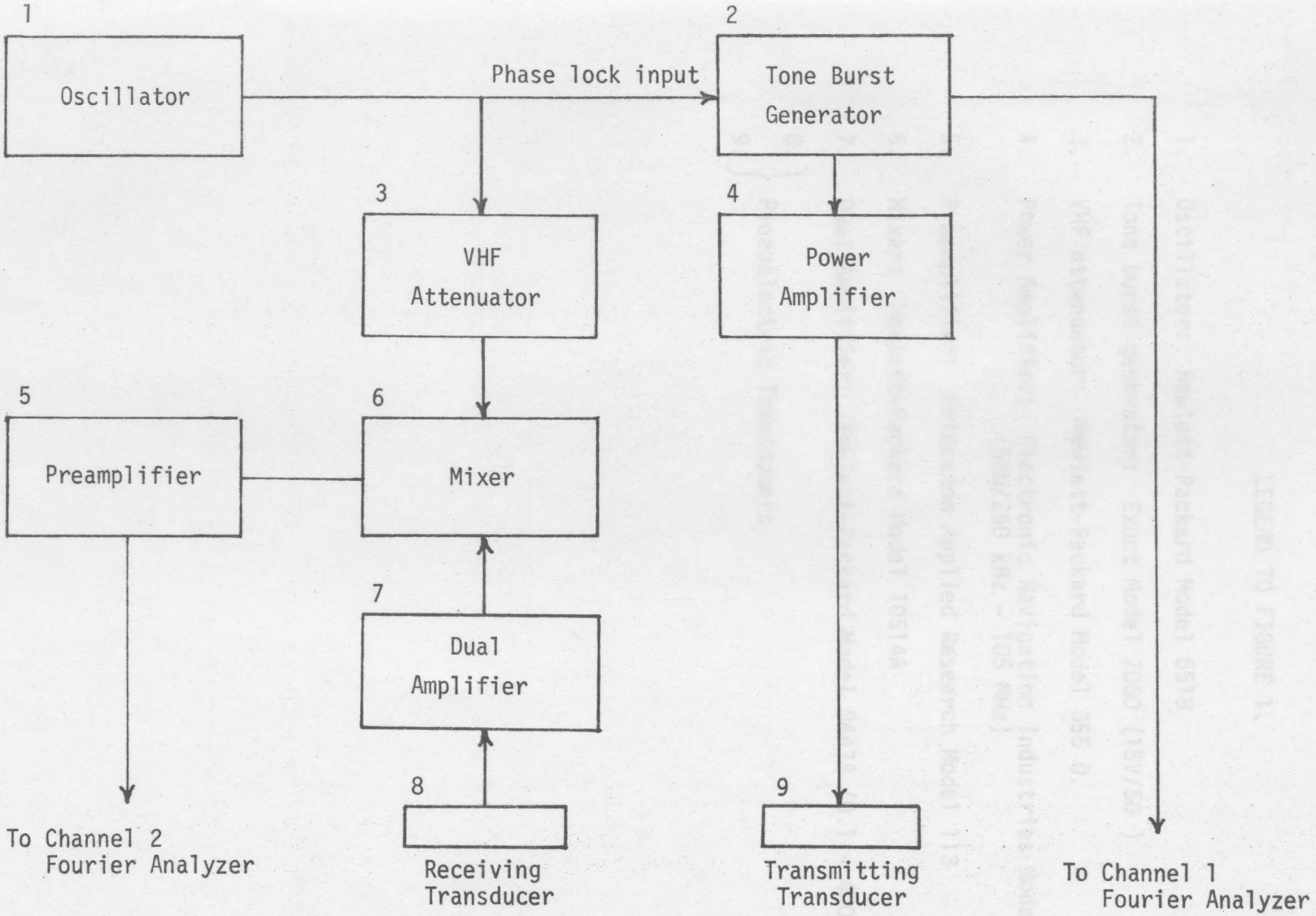

Figure 1

Block diagram of system for obtaining Ultrasonic Signature Analysis

LEGEND TO FIGURE 1.

1. Oscillator: Hewlett-Packard Model 6518
2. Tone burst generator: Exact Model 7060 (15V/50)
3. VHF attenuator: Hewlett-Packard Model 355 D.
4. Power Amplifier: Electronic Navigation Industries Model 3506 (50W/250 kHz - 105 MHz)
5. Preamplifier: Princeton Applied Research Model 113
6. Mixer: Hewlett-Packard Model 10514A
7. Dual Amplifier: Hewlett-Packard Model 8447A (0.1 - 400 MHz)
8. } Piezoelectric Transducers
9. }

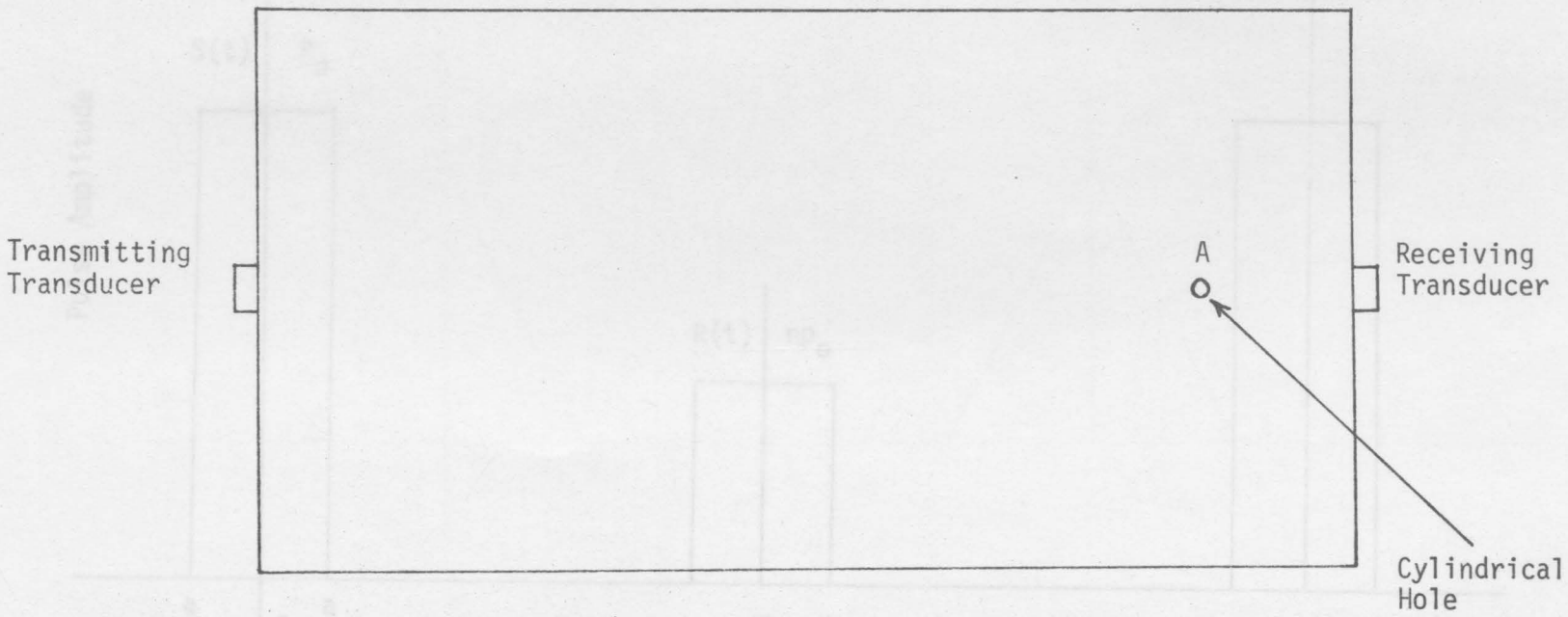

Figure 2

Experimental arrangement of transmitting and receiving transducers on an aluminum plate with a cylindrical hole

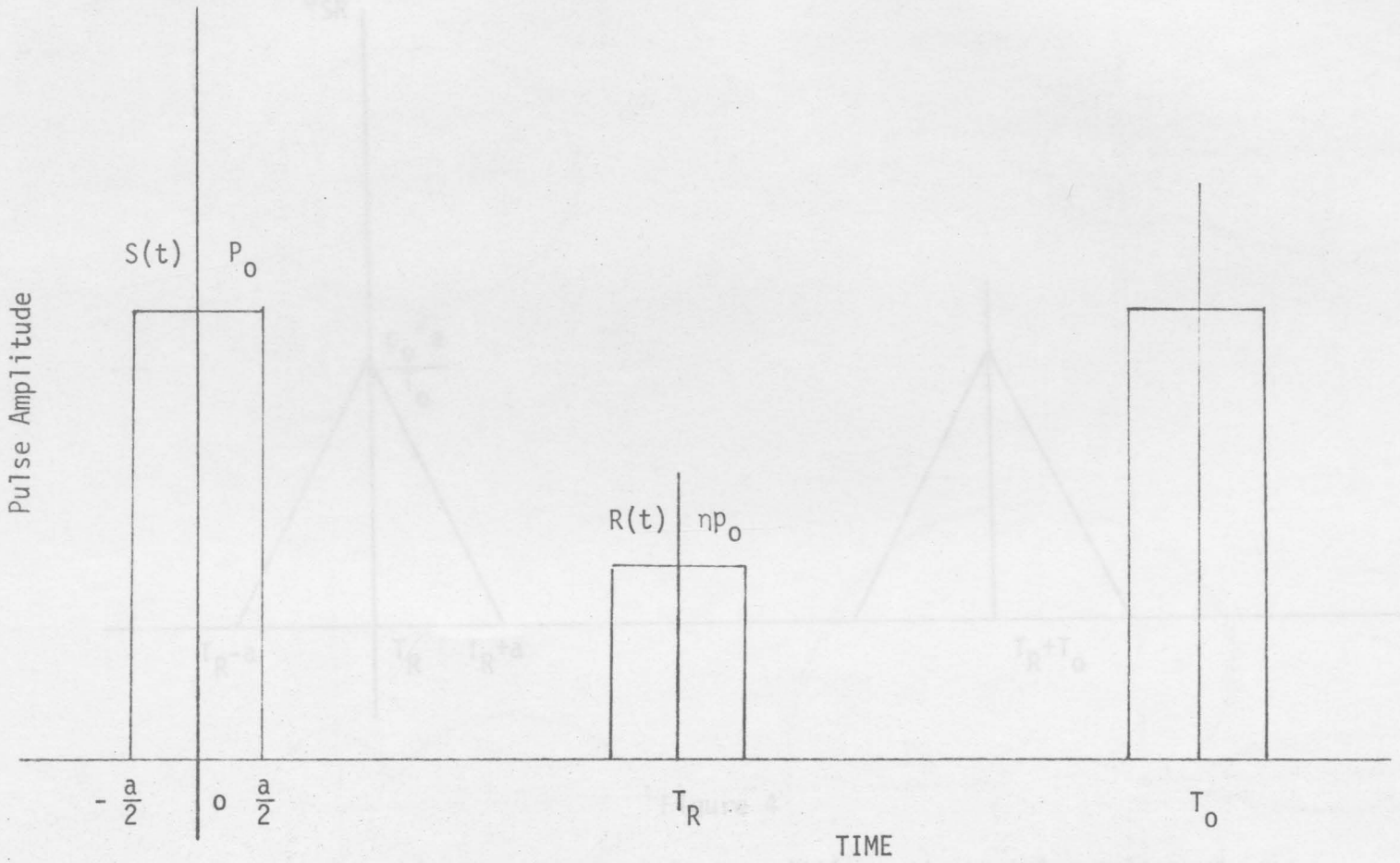

Figure 3

Transmitting pulse S(t) and receiving pulse R(t) vs. time

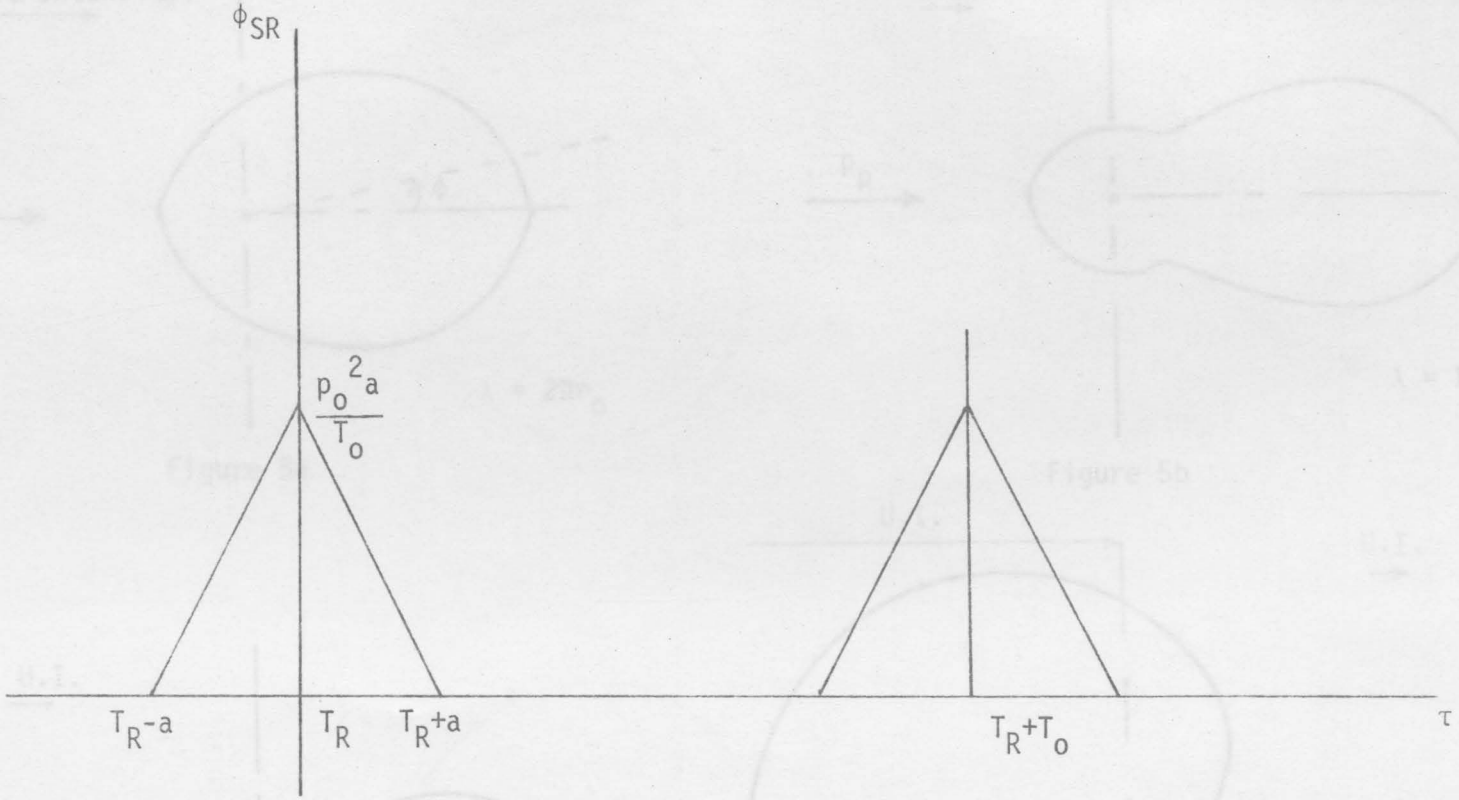

Figure 4

Cross-correlation function of transmitting and receiving pulses vs. τ

Far field radiation pattern of Ultrasonic Intensity

$|\psi_s(\phi)|^2$ vs. scattering angle ϕ

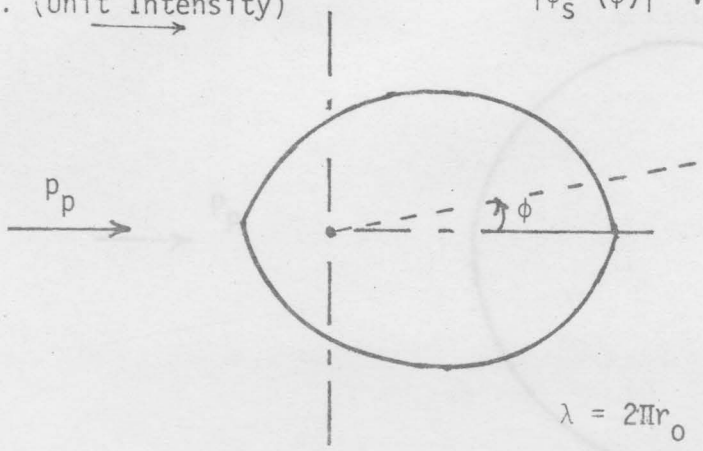

Figure 5a

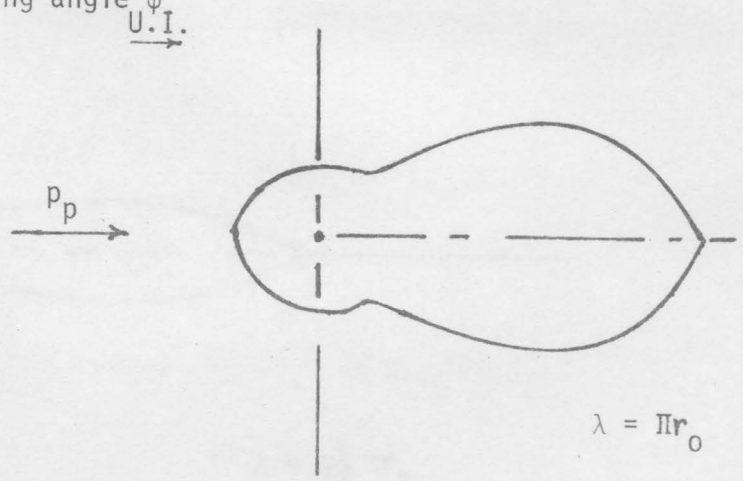

Figure 5b

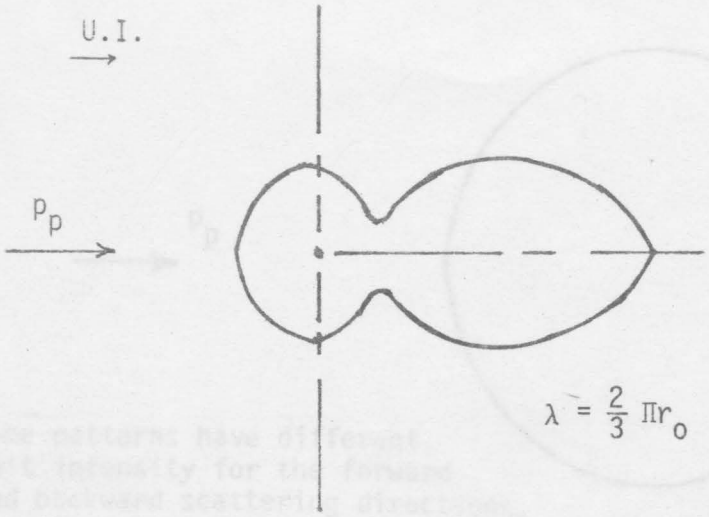

Figure 5c

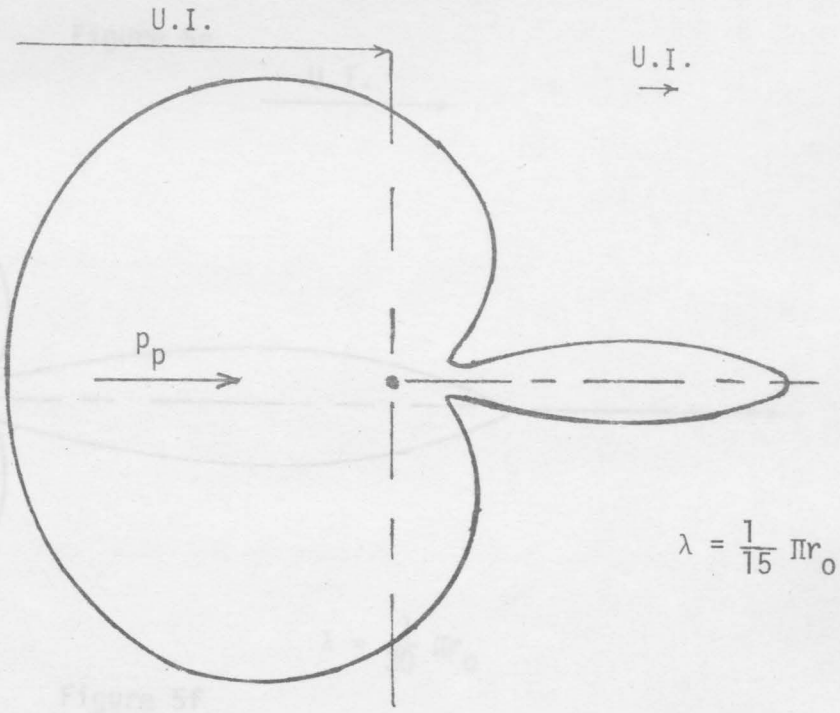

Figure 5d

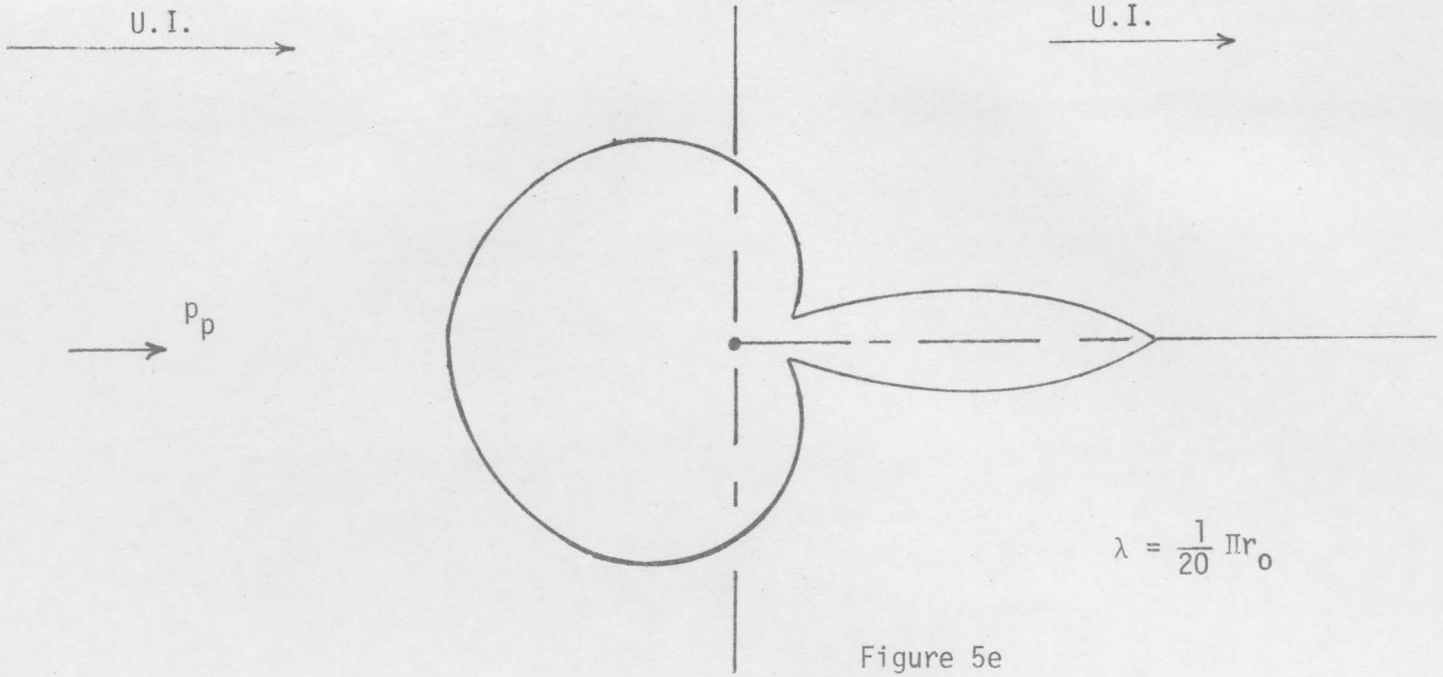

Figure 5e

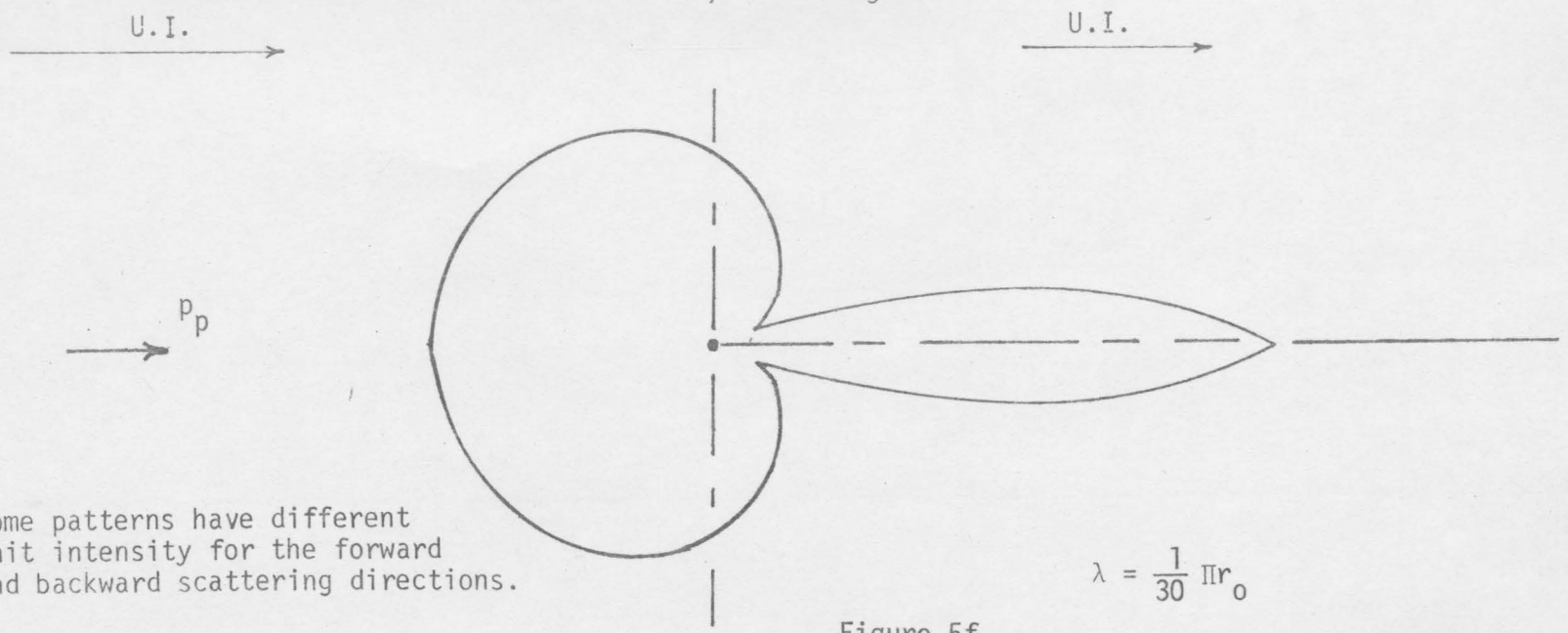

Figure 5f

Note: Some patterns have different unit intensity for the forward and backward scattering directions.